0026-895X/07/7205-1124–1131$20.00
MOLECULAR PHARMACOLOGY
Copyright © 2007 The American Society for Pharmacology and Experimental Therapeutics
Mol Pharmacol 72:1124–1131, 2007

Vol. 72, No. 5
37556/3263339
Printed in U.S.A.

2-Amino-*N*-{4-[5-(2-phenanthrenyl)-3-(trifluoromethyl)-1*H*-pyrazol-1-yl]-phenyl} Acetamide (OSU-03012), a Celecoxib Derivative, Directly Targets p21-Activated Kinase

Leonardo M. Porchia, Marcy Guerra, Yu-Chieh Wang, Yunlong Zhang, Allan V. Espinosa, Motoo Shinohara, Samuel K. Kulp, Lawrence S. Kirschner, Motoyasu Saji, Ching-Shih Chen, and Matthew D. Ringel

Division of Endocrinology, Department of Medicine (A.V.E., M.S., L.S.K., M.S., M.D.R.), and Division of Medicinal Chemistry and Pharmacognosy (L.M.P., M.G., Y.-C.W., Y.Z., S.K.K., C.-S.C.), the Ohio State University Colleges of Medicine and Pharmacy and the Arthur G. James Comprehensive Cancer Center, Columbus, Ohio

Received April 27, 2007; accepted August 2, 2007

ABSTRACT

p21-Activated kinases (PAKs) are regulators of cell motility and proliferation. PAK activity is regulated in part by phosphoinositide-dependent kinase 1 (PDK1). We hypothesized that reduced PAK activity was involved in the effects of 2-amino-*N*-{4-[5-(2-phenanthrenyl)-3-(trifluoromethyl)-1*H*-pyrazol-1-yl]-phenyl} acetamide (OSU-03012), a previously characterized PDK1 inhibitor derived from celecoxib. In three human thyroid cancer cell lines, OSU-03012 inhibited cell proliferation with reduced AKT phosphorylation by PDK1. OSU-03012 unexpectedly inhibited PAK phosphorylation at lower concentrations than PDK1-dependent AKT phosphorylation in two of the three lines. In cell-free kinase assays, OSU-03012 was shown to inhibit PAK activity and compete with ATP binding. In addition, computer modeling predicted a docking site for OSU-03012 in the ATP binding motif of PAK1. Finally, overexpression of constitutively activated PAK1 partially rescued the ability of motile NPA thyroid cancer cells to migrate during OSU-03012 treatment, suggesting that inhibition of PAK may be involved in the cellular effects of OSU-03012 in these cells. In summary, OSU-03012 is a direct inhibitor of PAK, and inhibition of PAK, either directly or indirectly, may be involved in its biological effects in vitro.

Phosphoinositide-dependent kinase 1 (PDK1) is an important regulator of 3-phosphoinositide-dependent cell signaling (Vanhaesebroeck and Alessi, 2000). Downstream effectors of PDK1, such as AKT (Meier and Hemmings, 1999), p70S6 kinase (Alessi et al., 1998), p21-activated kinases (PAK) (King et al., 2000), and atypical forms of protein kinase C (Dong et al., 1999) play critical roles as regulators of cellular proliferation, metabolism, apoptosis, and motility (Storz and Toker, 2002). Overactivation of PDK1-regulated pathways occurs commonly in cancer, and it has been associated with aggressive clinical behavior in some tumor types (Brader and Eccles, 2004). Therefore, there has been an interest in developing inhibitors of PDK1 and its effectors for cancer therapy.

OSU-03012 is a recently developed derivative of celecoxib that competitively inhibits PDK1 but not cyclooxygenase at low micromolar concentrations in vitro (Zhu et al., 2004). OSU-03012 has also been shown to induce cell death in prostate and breast cancer cell lines in an AKT-dependent manner and to have broad antitumor activity in vitro. Finally, this agent inhibits the growth of prostate and breast cancer xenografts in vivo and is well tolerated (Zhu et al., 2004; Kucab et al., 2005), suggesting that inhibition of PDK1 using OSU-03012 might have potential for anticancer therapy.

The global process of epithelial-to-mesenchymal transition (EMT) is common and mechanistically important in solid tumor progression (Thiery, 2002; Huber et al., 2005). Regu-

This work was supported by grants from the National Cancer Institute (R-01-CA102572-02 and R21-01-CA111461-01) to M.D.R.

Article, publication date, and citation information can be found at http://molpharm.aspetjournals.org.

doi:10.1124/mol.107.037556.

ABBREVIATIONS: PDK1, phosphoinositide-dependent kinase 1; PAK, p21-activated kinase; EMT, epithelial-to-mesenchymal transition; MBP, myelin basic protein; MTT, 3-(4,5-dimethylthiazol-2-yl)-2,5-diphenyl-2*H*-tetrazolium bromide; PARP, poly(ADP-ribose) polymerase; CA-PAK, constitutively active p21-activated kinase; FBS, fetal bovine serum; ELISA, enzyme-linked immunosorbent assay; PI3, phosphatidylinositol-3; DMSO, dimethyl sulfoxide; LY294002, 2-(4-morpholinyl)-8-phenyl-1(4*H*)-benzopyran-4-one hydrochloride; OSU-03012, 2-amino-N-{4-[5-(2-phenanthrenyl)-3-(trifluoromethyl)-1*H*-pyrazol-1-yl]-phenyl} acetamide; OSU-03013, 4-[5-(2-phenantrinenyl)-3-(trifluoromethyl)-1*H*-pyrazol-1-yl]-phenyl-guanidine.

latory pathways for EMT therefore represent important potential therapeutic targets for the stabilization and/or reversal of progressive cancer. PAKs are direct targets of PDK1 (King et al., 2000) that function as regulators of cell motility (Kumar et al., 2006) and EMT (Yang et al., 2005). Thus, inhibition of PDK1-mediated PAK activation represents a potential therapeutic approach to cancer therapy.

Activation of PAKs is required for the formation and stabilization of the leading edges of cells that result in directional motility (Sells et al., 2000). The generation of dynamic motility-related structures at focal adhesions is regulated in part by small GTPases in the Rho family, such as Rac and cdc42 (Sahai and Marshall, 2003; Burridge and Wennerberg, 2004; Zhao and Manser, 2005), and other pathways. GTP-bound Rac and cdc42 bind to specific sites in the N-terminal p21-binding domain of PAK, resulting in the subsequent release of PAK from its autoinhibited state (Lei et al., 2000) maintained by binding to PAK-interacting exchange factor (Rac/cdc42 GEF6). Once released from PAK-interacting exchange factor binding, PAK requires phosphorylation of several residues for activation, including autophosphorylation at Ser144 (Gatti et al., 1999; Chong et al., 2001) and phosphorylation by PDK1 at Thr423 (King et al., 2000), the latter of which is critical for maximal activation of the protein. Thr423 is also reported to be a PAK autophosphorylation site (Zenke et al., 1999).

In the present study we demonstrate that OSU-03012 inhibits both AKT and PAK activity and is cytotoxic in three thyroid cancer cell lines. OSU-03012 unexpectedly reduced levels of phosphorylated PAK occurred at concentrations lower than those required to block PDK1-mediated AKT phosphorylation in two of the examined lines. Subsequent studies demonstrate that OSU-03012 directly inhibits PAK kinase activity with an IC_{50} value of ~1 μM. Overexpression of constitutively activated PAK1 cDNA partially rescued the ability of the most motile cell line (NPA) examined to migrate in the presence of OSU-03012, suggesting that PAK inhibition, either directly or indirectly, is involved in the biological effects of the compound in these cells.

Materials and Methods

Reagents and Vectors. Anti-AKT, anti-phospho-AKT (Ser473), anti-PAK1/2/3, anti-phospho-Thr423 PAK, and anti-Myc antibodies were purchased from Cell Signaling Technology (Danvers, MA). Anti-poly(ADP-ribose) polymerase (PARP) antibody was obtained from Santa Cruz Biotechnology (Santa Cruz, CA), anti-Vimentin was obtained from Sigma-Aldrich (St. Louis, MO.), anti-phospho-Ser56-vimentin was obtained from Medical and Biological Laboratories (Woburn, MA), and anti-glyceraldehyde-3-phosphate dehydrogenase was obtained from Novus Biologicals (Littleton, CO). Expression vectors containing myc-tagged constitutively activated PAK1 cDNA was the generous gift of Dr. Jonathan Chernoff (Fox Chase Cancer Center, Philadelphia, PA) (Sells et al., 1997, 1999). All other reagents were obtained from Sigma-Aldrich unless otherwise noted.

Cell Culture and Transient Transfection of Plasmids. Human thyroid carcinoma NPA (papillary) (Fagin et al., 1993), WRO (follicular) (Estour et al., 1989), and ARO (anaplastic) cell lines (Fagin et al., 1993) were obtained from Dr. Guy Juillard (University of California, Los Angeles, Los Angeles, CA) and were grown in RPMI 1640 medium (Invitrogen, Carlsbad, CA) supplemented with 10% fetal bovine serum (FBS), 100 mM L-glutamine, and 100 μM Nonessential Amino Acids (Invitrogen). Once the cells achieved 70% confluence, the cells were washed, trypsinized, and replated. The growth medium was replaced with RPMI 1640 containing either 0.2 or 5% FBS, as noted for individual experiments for 24 h, and this medium was aspirated and replaced with fresh RPMI 1640 with the same FBS concentration containing OSU-03012 or vehicle. For transfection studies, NPA cells were seeded 16 h before transfection at ~20% confluence. Cells were transfected using Lipofectamine plus transfection reagent (Invitrogen) according to the manufacturer's protocol. Transfection efficiency was estimated by cotransfection with phosphorylated enhanced green fluorescent protein (Clontech, Mountain View, CA).

Cell Proliferation. NPA, WRO, and ARO cells were seeded into six-well plates at ~150,000 cells/well in RPMI 1640 containing 10% FBS. After the 24-h attachment period, cells were treated with the indicated concentration of OSU-03012 or DMSO vehicle in RPMI 1640 containing 5% FBS. At different time intervals, cells were harvested by trypsinization and counted using a Coulter counter model Z1 D/T (Beckman Coulter, Fullerton, CA). Triplicates were performed in all experiments, and experiments were performed on three occasions. The concentration of OSU-03012 required to inhibit growth by 50% (GI_{50}) was calculated using the guidelines suggested by the National Institutes of Health.

Cell Viability Analysis. The effect of OSU-03012 on cell viability was assessed by using the 3-(4, 5-dimethylthiazol-2-yl)-2, 5-diphenyl-2*H*-tetrazolium bromide (MTT) assay. Triplicates were performed in each individual experiment, and experiments were repeated at least three separate times. Cells were grown in 96-well plates for 24 h and were exposed to various concentrations of OSU-03012 dissolved in DMSO (final concentration $\leq$ 0.1%) in RPMI 1640 containing 5% FBS. The medium was removed and replaced by 200 μl of 0.5 mg/ml MTT in RPMI 1640 with 10% FBS according to the manufacturer's recommended protocol (T.C.I. America, Portland, OR), and cells were incubated in the CO_2 incubator at 37°C for 2 h. Supernatants were removed from the wells, and the reduced MTT dye was solubilized in 200 μl of DMSO per well. Absorbance at 570 nm was determined on a plate reader. The IC_{50} value was calculated using CalcuSyn (versio 1.2; Biosoft, Ferguson, MO).

Cell Cycle Analysis. NPA, WRO, and ARO cells were treated with OSU-03012 for 24 h in RPMI 1640 containing 5% FBS. All cells were collected, and 1×10^6 cells were centrifuged, resuspended in ice-cold 70% ethanol, and stored at −20°C until analysis. Washed cells were stained in 0.1% Triton X-100 in phosphate-buffered saline with 1 μg/ml propidium iodide (Sigma-Aldrich) and RNase A (Invitrogen). Flow cytometry was performed using a flow cytometer (BD FACSCalibur; BD Biosciences) with a 610 long-pass filter for data collection. Data were filtered, and cell cycle phases were quantified using the Modfit program (Verity Software, Bowdoin, ME). Duplicates were performed in all experiments, and experiments were performed on three occasions.

PAK Kinase Assay. Recombinant active PAK 1 (Cell Signaling) with various concentrations of OSU-03012 or 0.1% DMSO was incubated in the presence or absence of MBP (Upstate Biotechnology, Charlottesville, VA) in a 1× kinase buffer (Cell Signaling). The addition of [γ-^{32}P]ATP (2.5 μCi/reaction or 5 μCi/100 μM unlabeled ATP) (GE Healthcare, Chalfont St. Giles, Buckinghamshire, UK) started the reaction, which was incubated at 30°C for 30 min. The reaction was terminated by the addition of EDTA. The phosphorylated MBP was separated from the residual [γ-^{32}P]ATP using P81 phosphocellulose paper and quantified by a scintillation counter after three washes with 0.75% phosphoric acid. Results were also verified after visualization of ^{32}P-labeled MBP after separation on 12% polyacrylamide gel electrophoresis and autoradiography. For the Lineweaver-Burk plot analysis, the ratio of radioactive ATP to nonradioactive ATP was not altered. The IC_{50} values are the means of five independent experiments quantified using P81 phosphocellulose paper performed in duplicate and were calculated using CalcuSyn (version 1.2; Biosoft). Additional experiments (n = 3) were performed as described above using OSU-03013, another celecoxib derivative with PDK1 inhibitory effects (Zhu et al., 2004)

Protein Extraction and Immunoblotting. Protein extraction and immunoblotting were performed as described previously in detail (Vasko et al., 2004; Saji et al., 2005). After cells were washed with ice-cold phosphate-buffered saline, cells were collected, centrifuged for 5 min at 500*g*, and washed with 500 μl of ice-cold Tris-buffered saline. Cell lysis or M-PER buffer (Pierce Biotechnology, Inc., Rockford, IL) supplemented with 0.3 μM okadaic acid and 1 μg/ml each of aprotinin, pepstatin, leupeptin, and 20 mM 4-amidinophenyl methane-sulfonyl fluoride were added to the tubes, which were incubated on ice for 15 min. The cells were centrifuged at 16,000*g* for 10 min at 4°C, and the supernatant was saved and stored at −80°C. Protein concentrations were calculated using Micro BCA Protein Assay Kit (Pierce). Relative quantitation of proteins was determined using ImageGauge software (Fuji Photo Film Co., Tokyo, Japan).

Apoptosis Analysis. To assess apoptosis, Cell Death Detection ELISA kit (Roche Diagnostics, Indianapolis, IN) for nucleosome detection and immunoblot analysis for cleaved PARP were performed. The ELISA was performed according to the manufacturer's instructions. In brief, 8×10^5 NPA, WRO, and ARO cells were cultured in a T-25 flask for 24 h before treatment. Cells were treated with the DMSO vehicle or OSU-03012 at the indicated concentrations in RPMI 1640 containing 5% FBS for 24 h, collected, and cell lysates equivalent to 1×10^4 cells were used in the ELISA. Triplicates were performed in all experiments, and experiments were performed on three occasions. For the PARP cleavage assay, cellular proteins from cells treated with OSU-03012 in the same conditions described above were used to detect fragmented PARP by immunoblotting with anti-PARP antibody.

Migration Assays. Migration assays were performed as described previously in detail (Vasko et al., 2004; Saji et al., 2005) NPA cells were grown in RPMI 1640 containing 10% FBS. After 24 h, the medium was aspirated, and RPMI 1640 containing 0.2% FBS was added for 24 h. The cells were trypsinized for 2 to 5 min, washed, and resuspended in RPMI 1640 containing 0.2% FBS. The cell concentration was calculated by hemocytometer. Four hundred microliters of 0.2% FBS medium was added into 24-well plates, and a Boyden chamber (8-μm pore) was inserted into each well. NPA cells (9×10^5) were added to each insert, and the NPA cells were allowed to attach in an incubator at 37°C at 5% CO_2 for 30 min. The inserts were switched to a new well containing RPMI 1640 containing 5% FBS. OSU-03012 or vehicle was added to the upper chamber, and the chamber was incubated for 24 h. Cells were visualized by Diff-Quik (Dade Behring Inc., Newark, DE) staining before and after swiping the top of the membranes, allowing for the determination of total cells and the number of cells on the bottom of the membrane as described previously. Experiments were performed on at least three occasions.

Computer Modeling. The three-dimensional structure of OSU-03012 was generated and minimized, using MMFF94 force field, by SYBYL 7.1 software (Tripos Associates, St. Louis, MO). The crystal structure of PAK1 kinase with two mutations (entry code 1YHV, K299R, T423E; Lei et al., 2005) was retrieved from the Research Collaboratory for Structural Bioinformatics Protein Data Bank (Berman et al., 2000). The heteroatom entries were deleted, and residue 299 was modified from arginine into lysine in 1YHV. The protein structure was then subjected to the addition of polar hydrogens, Kollman charges, and solvation parameters using the molecular modeling software "AutoDock Tools" as described previously (Goodsell and Olson, 1990). Gasteiger charges and rotatable bonds of OSU-03012 were assigned with default parameters. The structure of ATP was extracted from the crystal structure of phosphorylase kinase (Protein Data Bank accession code 2PHK) and was assigned Gasteiger charges. The torsions of ATP were defined as 0. The grid parameter file of 1YHV was generated on the well-defined ATP binding domain, and the default parameters in AutoDock Tools were used. The docking parameter files of OSU-03012 and ATP were defined with GA runs [100], population size [150], and evaluations [5×10^7] using the Lamarckian genetic algorithm. Other default parameters were used. Docking was performed with AutoDock 3.05 (Rosenfeld et al., 2003) using the Pentium 4 Cluster at Ohio Supercomputer Center (available at http://www.osc.edu).

Statistical Analysis. All quantitative data are represented as mean ± S.D. Analysis was performed using GB-STAT version 10.0. The significance of differences between groups was examined by analysis of variance and post hoc analysis or by Dunnett's test if the distribution was normal. Statistical significance was a P value of <0.05.

Results

OSU-03012 Inhibited Thyroid Cancer Cell Proliferation and Induced Apoptosis. To investigate whether OSU-03012 inhibited thyroid cancer cell proliferation, NPA, WRO, and ARO cells derived from poorly differentiated human papillary, follicular, and anaplastic thyroid cancer, respectively, were treated with OSU-03012 at 2.5 to 10 μM concentrations for 1, 2, and 3 days. Compared with vehicle-treated cells, OSU-03012 inhibited proliferation of all cell lines. Moreover, OSU-03012 seemed to be cytotoxic at higher concentrations, as shown by the decrease in cell number below the original number that was plated (Fig. 1A). These cell-counting data were confirmed using an MTT assay (data not shown). The GI_{50} and IC_{50} concentrations after 24 h of treatment were 1.29 ± 0.10 and 3.18 ± 0.80 for NPA, 2.16 ± 0.09 and 6.53 ± 1.57 for WRO, and 2.10 ± 0.22 and 5.91 ± 0.92 μM for ARO cells, respectively.

To determine the effects of OSU-03012 on thyroid cancer cell cycle progression and to compare its effects with PI3 kinase inhibition, NPA, WRO, and ARO cells were treated with OSU-03012 or LY294002, a PI3 kinase inhibitor, for 24 h. Cells were labeled with propidium iodide, and flow cytometry was performed. LY294002 induced cell cycle arrest in G_1/S phase beginning at 12.5 μM (data for 25 μM shown in Fig. 1B), as has been reported previously (Motti et al., 2005). In contrast, OSU-03012 treatment resulted in an increase of cells in S phase without an increase of cells in G_2 in a dose-responsive manner beginning at 1 μM (Fig. 1B). These data suggest that the antiproliferative mechanisms between these two agents differ.

To determine whether the cytotoxic effects of OSU-03012 (Fig. 1A) were associated with apoptosis, Western blots were performed to detect PARP cleavage. OSU-03012 treatment induced PARP cleavage in all three cell lines (Fig. 1C), confirming that OSU-03012 induces apoptosis in these cells. The amount of PARP cleavage varied between the three cell lines and correlated with the quantitative results detecting nucleosome release by ELISA (data not shown). Thus, it seems likely that apoptosis is not responsible for all OSU-03012-induced cell death in thyroid cancer cells. Nearly 100% of NPA and ARO cells died after exposure to 10 μM OSU-03012 (Fig. 1A).

OSU-03012 Inhibited AKT and PAK Phosphorylation in Thyroid Cancer Cells. NPA, WRO, and ARO cells were treated with OSU-03012 or vehicle for 24 h. Western blots were performed using anti-Thr308 phospho-AKT, anti-total AKT, and anti-glyceraldehyde-3-phosphate dehydrogenase primary antibodies. The anti-phospho-Thr308 AKT antibody was chosen because this is a PDK1-specific phosphorylation site. OSU-03012 treatment resulted in reduced AKT phosphorylation by PDK1, consistent with its known inhibitory

effect on this kinase (Fig. 2). The dose required varied among the cell lines.

The ability of OSU-03012 to inhibit PDK1-dependent PAK phosphorylation was assessed by Western blot for Thr423 phospho-PAK (Fig. 2). In WRO and NPA cells, OSU-03012 reduced Thr423 phospho-PAK levels at lower concentrations than inhibition of AKT phosphorylation in comparison with vehicle alone (zero concentration lane). Vimentin is a downstream target of PAK involved in intermediate filament organization and cell motility that is expressed in NPA but not WRO or ARO cells (Vasko et al., 2007). Using an antibody for PAK-dependent phosphorylation of vimentin at the Ser56 residue, OSU-03012 reduced vimentin phosphorylation in concert with reduced PAK phosphorylation, consistent with reduced PAK activity (Fig. 2C).

OSU-03012 Directly Inhibited PAK Activity via Competitive Inhibition of ATP Binding. Because OSU-03012 inhibited PAK phosphorylation at lower concentrations than PDK-1-dependent AKT phosphorylation in two cell lines, and because the Thr423 in PAK is reported to be both a PDK1 and PAK autophosphorylation site, we questioned whether OSU-03012 might also directly inhibit PAK. Recombinant PAK1 protein was incubated with MBP, a known substrate of PAK1, in the presence of increasing concentrations of OSU-03012. Representative autoradiographic data from one of several initial dose-response experiments is shown in Fig. 3A. These experiments suggested the IC_{50} value of OSU-03012 for PAK was between 500 nM and 1 μM. To define the IC_{50} value, five subsequent PAK kinase assays were performed using P81 paper for quantitation (Fig. 3B). Using this assay, OSU-03012 reduced PAK activity with an IC_{50} value of 1.03 $\pm$ 0.59 μM. Subsequent kinetic experiments demonstrated an inverse relationship between the effect of OSU-03012 on PAK activity and ATP concentration. The K_m value of PAK for ATP was calculated to be 27 μM. The Lineweaver-Burk plot of these data suggests that OSU-03012 is a competitive inhibitor of ATP binding to PAK (Fig. 3C). OSU-03013 is another derivative of celecoxib that is structurally similar to OSU-03012 and also inhibits PDK-1 (Zhu et al., 2004). Similar to OSU-03012, the OSU-03013 inhibited PAK kinase activity with an IC_{50} value of 0.81 $\pm$ 0.56 μM. Further cellular studies were not pursued with this agent because of toxicity in vivo (C.-S. Chen, unpublished observations).

We next performed molecular modeling to determine potential binding sites of OSU-03012 in the ATP binding domain of PAK1. Because the PAK1 crystal structure complexed with ligand is not available, we modified the double mutant 1YHV (K299R, T432E), for which a crystal structure is known, to undertake docking. This model was chosen because it has been demonstrated to adopt an essentially active conformation (Lei et al., 2000). We modified the Arg299 back to the wild-type Lys299 in 1YHV and hypothesized that this would represent the active conformation of PAK1. To test this hypothesis and to compare the binding modes of ATP and OSU-03012, the coordinates of ATP in 2PHK (see *Materials and Methods*) were retrieved and were rigidly docked into the modified PAK1 structure with no rotatable bonds allowed in ATP. The binding mode of ATP is shown in Fig. 4A, in which ATP is docked into the ATP binding pocket of PAK1. As in other kinases, ATP is predicted to form two hydrogen bonds with Ala297 and Lys299. In addition, the 5′-OH group of the ATP sugar moiety forms a hydrogen bond with Glu315. An ionic bond links the α-phosphate group of ATP and terminal amino group of Lys299.

The docking results suggest a potential site for OSU-03012 interactions with the ATP binding domain of PAK1 (Fig. 4B). Only one potential docking mode was found, and this mode was similar to that reported previously for the interaction of OSU-03012 with PDK1 (Zhu et al., 2004). In this model, two hydrogen bonds are predicted to form between the terminal amino group of OSU-03012 and Ala297 and Val342. The phenanthrene ring of OSU-03012 interacts with residues

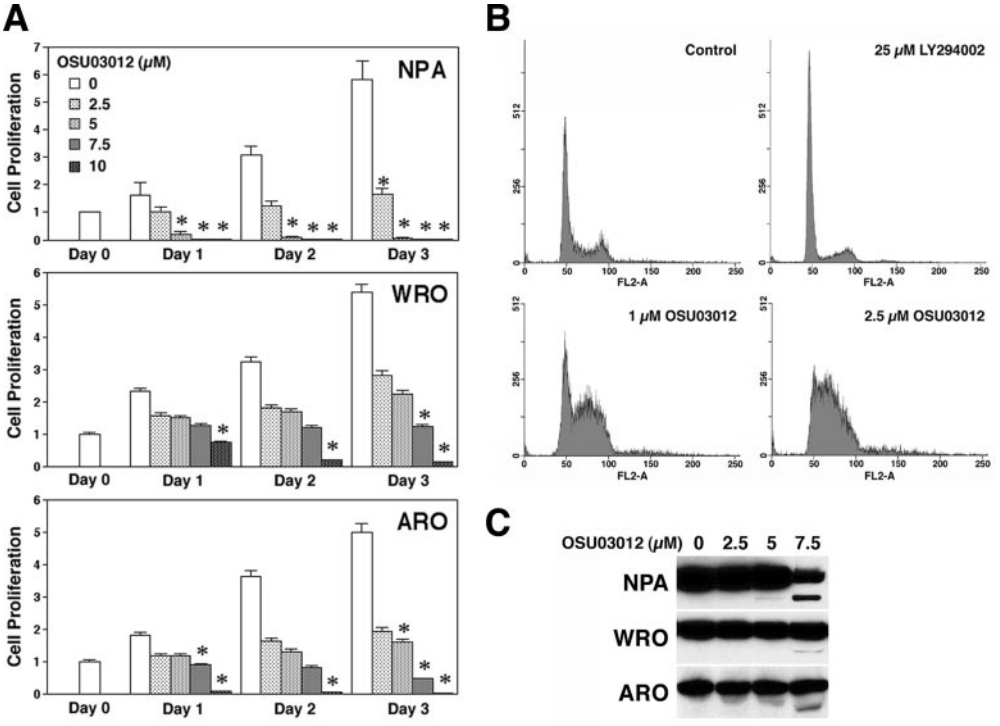

Fig. 1. OSU-03012 decreases cell viability and increases cells in S phase. A, NPA, WRO, and ARO were treated with increasing doses of OSU-03012 for 0, 24, 48, and 72 h and then counted. OSU-03012 caused a decrease in cell numbers in each cell line (*, $P < 0.01$). The y-axis represents arbitrary units with the number of cells normalized to day 0 (pretreatment), which is set at 1.0. Mean values and S.D. are shown. B, NPA cells were treated with 1 and 2.5 μM OSU-03012 or 25 μM LY294002 for 24 h. Cells were collected and stained with propidium iodine and then analyzed by flow cytometry. OSU-03012 caused a dose-related increase in the number of cells in the S phase, whereas LY294002 blocked G_1/S transition. Representative data are shown. Similar results were noted in replicate experiments and with the ARO and WRO cell lines (data not shown). C, Western blot for PARP demonstrates PARP cleavage in all three cell lines beginning at 5 μM for NPA cells and 7.5 μM for WRO and ARO cells.

Leu311, Ile312, and Lys308 through hydrophobic interactions. In addition, the model predicts an important π-cation interaction between the protonated terminal amino group of Lys299 and the 2-phenyl group in OSU-03012 with a distance of approximately 4 Å (Scrutton and Raine, 1996).

OSU-03012 Inhibited Thyroid Cancer Cell Migration in a PAK-Dependent Manner. Because of the central role of PAK in cell motility, we next investigated whether OSU-03012 was able to decrease thyroid cancer cell migration. For these experiments, we focused on the NPA cells because they are more motile than the other cell lines in this assay system and demonstrate mesenchymal phenotype (Vasko et al., 2007). Initial experiments demonstrated that a statistically significant reduction in migration was detected beginning between 1 and 2.5 μM OSU-03012 compared with DMSO control (data not shown, but see control vector experiments in Fig. 5, A and B).

To determine whether this effect was PAK-dependent, NPA cells were transfected with a constitutively activated PAK cDNA (CA-PAK) or control vector. Expression of CA-PAK was confirmed by Western blot (Fig. 5D). Cell migration was examined in the presence of OSU-03012 (1–5 μM) or vehicle for 24 h. 1, 2.5, and 5 μM OSU-03012 reduced the migration of vector-transfected cells compared with vehicle-treated cells ($P < 0.05$, Fig. 5, A and B). In preliminary experiments, lower concentrations of OSU-03012 (<1 μM) minimally inhibited migration of NPA cells, but this was not statistically significant (data not shown). Overexpression of CA-PAK in NPA cells reduced the ability of OSU-03012 to block cell migration, as demonstrated by a shift in the dose-response so that only the 5 μM dose blocked migration (Fig. 5B; $P < 0.05$), consistent with a partial rescue effect. Moreover, the level of cell migration in CA-PAK transfectants was statistically different from that of controls at both the 1 and 2.5 μM doses ($P < 0.01$). Transfection efficiency was approximately 30% as estimated by cotransfection of a green fluorescent protein-expressing plasmid.

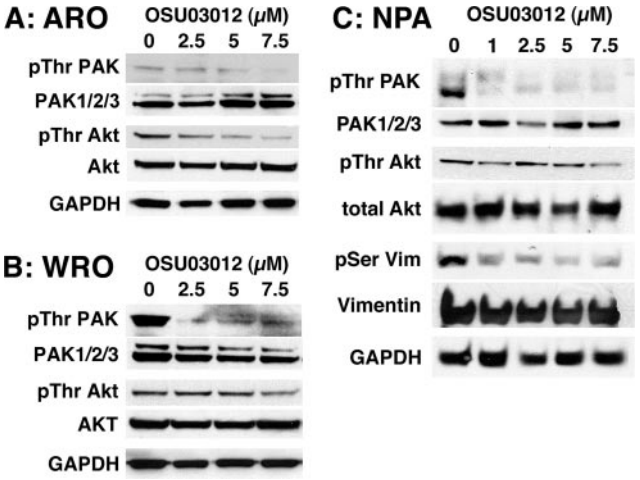

Fig. 2. OSU-03012 decreases AKT and PAK phosphorylation. ARO, WRO, and NPA cells were incubated with OSU-03012 or DMSO alone (0 μM) at increasing concentrations for 24 h. Whole-cell lysates were isolated, and Western blots were performed. Representative data are shown and demonstrate that OSU-03012 inhibits PDK-1 dependent Thr308 AKT phosphorylation and Thr423 PAK phosphorylation. In NPA cells, the only line that expressed vimentin, PAK-dependent vimentin phosphorylation at Ser56 was also reduced by OSU-03012. These data are representative of experiments performed in triplicate.

Discussion

In the present study, we demonstrate that the celecoxib derivative OSU-03012 is a direct inhibitor of PAK kinase. OSU-03012 was developed from celecoxib and was established to be a PDK-1 inhibitor at low micromolar concentrations with the ability to inhibit proliferation and induce apoptosis in an AKT-dependent manner based on rescue experiments using constitutively activated AKT (Kulp et al., 2004; Zhu et al., 2004). Consistent with these data, we demonstrate that OSU-03012 is able to decrease proliferation and increase apoptosis in three thyroid cancer cell lines in concert with inhibition of PDK1-dependent AKT phosphorylation. Moreover, we demonstrate that OSU-03012 seems to induce S-phase arrest in these lines in contrast to the effects of the PI3 kinase inhibitor, LY294002. The precise mechanism for this effect is uncertain and requires investigation in a larger number of cell lines, but it could include inhibition of PDK-1, PAK, and/or other targets not yet defined that might vary between cell systems.

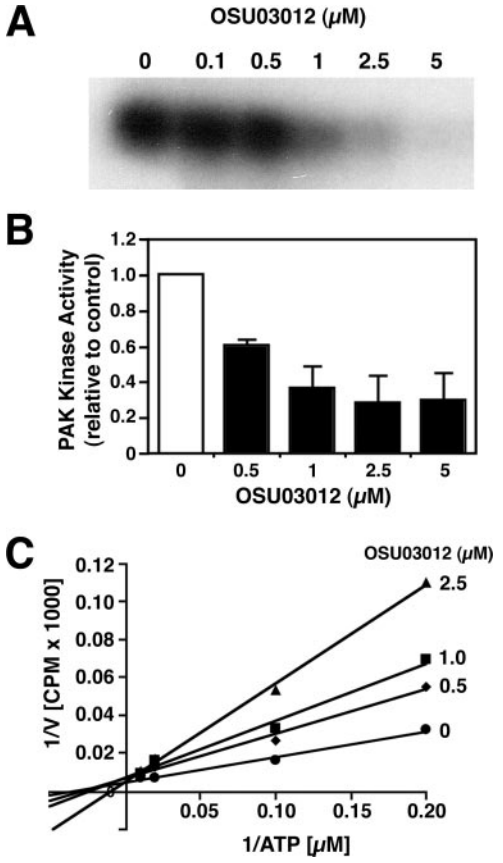

Fig. 3. OSU-03012 directly inhibits PAK through direct competition with ATP. A, in vitro recombinant PAK1 kinase assay using MBP as substrate demonstrates a dose-dependent reduction of p-MBP levels by OSU-03012, as determined by autoradiography. The inhibitory effect occurs at doses greater than 0.5 μM. Data from one representative experiment are shown. B, five quantitative assays using P81 paper were performed to define the inhibitory range of OSU-03012 for PAK activity. Using these data, the IC_{50} value was calculated to be 1.03 ±.59 μM. Results from all experiments are shown as mean values with S.D. shown as error bars. C, Lineweaver-Burk plot of the competition of OSU-03012 with ATP using PAK1 kinase assay. One representative experiment is shown. Substrate specificity was determined using an ATP concentration range of 5 to 100 μM in the presence of increasing concentrations of OSU-03012; the K_m value of PAK for ATP was determined to be 27 μM in multiple experiments.

As shown in Fig. 3, OSU-03012 directly inhibits PAK1 kinase activity through competitive inhibition of ATP binding. This finding is supported by computer-based molecular modeling, which suggests a potential binding site for OSU-03012 in the ATP binding region of PAK1 (Fig. 4). It should be noted that the AutoDock software used predicts a higher binding affinity for OSU-03012 than ATP, which is consistent with the experimental data by comparing the K_m value of PAK1 for ATP (27 μM) and the IC_{50} value of OSU-03012 (1.03 μM). These data, in addition to the similarity between the predicted docking modes of OSU-03012 for PAK1 and PDK-1, suggest a common mechanism of action that might account for its multikinase inhibitory effects. In addition, OSU-03012 was submitted to a commercial kinase-profiling service (Upstate) to screen for activity against a panel of kinases, including Akt, CDK7/cyclin H, IκB kinase complex b, protein kinase A, p70S6K, protein kinase Cγ, mitogen-activated protein kinase kinase 1, mitogen-activated protein kinase 2, platelet-derived growth factor receptor α, c-RAF, and cSrc. In this screening assay, none of these kinases was inhibited by OSU-03012 at 10 μM (data not shown). Although it is recognized that the panel is not exhaustive and that OSU-03012 may have activity against other kinases, the absence of activity at 10 μM in this screening assay suggests a degree of specificity for OSU-03012.

Because PAKs play an important role in cell motility and because OSU blocks both PDK1 and PAK activity, we hypothesized that the ability of OSU-03012 to inhibit cell motility would depend in part on its ability to inhibit PAK. We focused on the NPA cells because of their high migratory capacity in Boyden chamber assays. Indeed, the ability of OSU-03012 to inhibit motility in these cells seems to partially depend on its inhibition of PAK activity, as determined in the rescue experiments using the constitutively activated PAK cDNA. These data are further supported by the observation that OSU-03012 inhibits PAK phosphorylation of vimentin, a regulator of EMT and migration in these cells (Vasko et al., 2007), at doses similar to the antimotility effects of the compound. Thus, it seems that the effect of OSU-03012 on migration depends, at least in part, on PAK inhibition in NPA cells, which could occur by inhibition of both PAK and PDK1. The rescue experiments with the PAK1 constructs serve as "proof of principle" to demonstrate that the inhibition of PAK is involved in the biological effects of OSU-03012 in NPA cells. It is not yet clear whether the anti-PAK effect in the NPA cells occurs primarily via inhibition of PDK1, PAK, or both. In addition, they do not exclude a potential role for other OSU-03012 targets in its effects. Therefore, further studies are required to determine the relative and more generalized importance of PAK inhibition in comparison with other OSU-03012-targeted pathways on migration, proliferation, and/or apoptosis in multiple cell lines with different genetic backgrounds.

There are six known isoforms of PAKs. PAKs 1 to 3 share similar modes of activation (GTPase-dependent) and a high degree of sequence homology in the regulatory and kinase domains. In contrast, PAKs 4 to 6 have GTPase-independent modes of activation and share less sequence homology with PAKs 1 to 3 (Hofmann et al., 2004). The ability of OSU-03012 to block isoform-specific kinase activity is an area of active investigation but seems unlikely based on the sequence homology of PAKs 1 to 3 in the kinase domain.

The literature demonstrating a role for PAK activity in directional cell motility and EMT is supported by recent

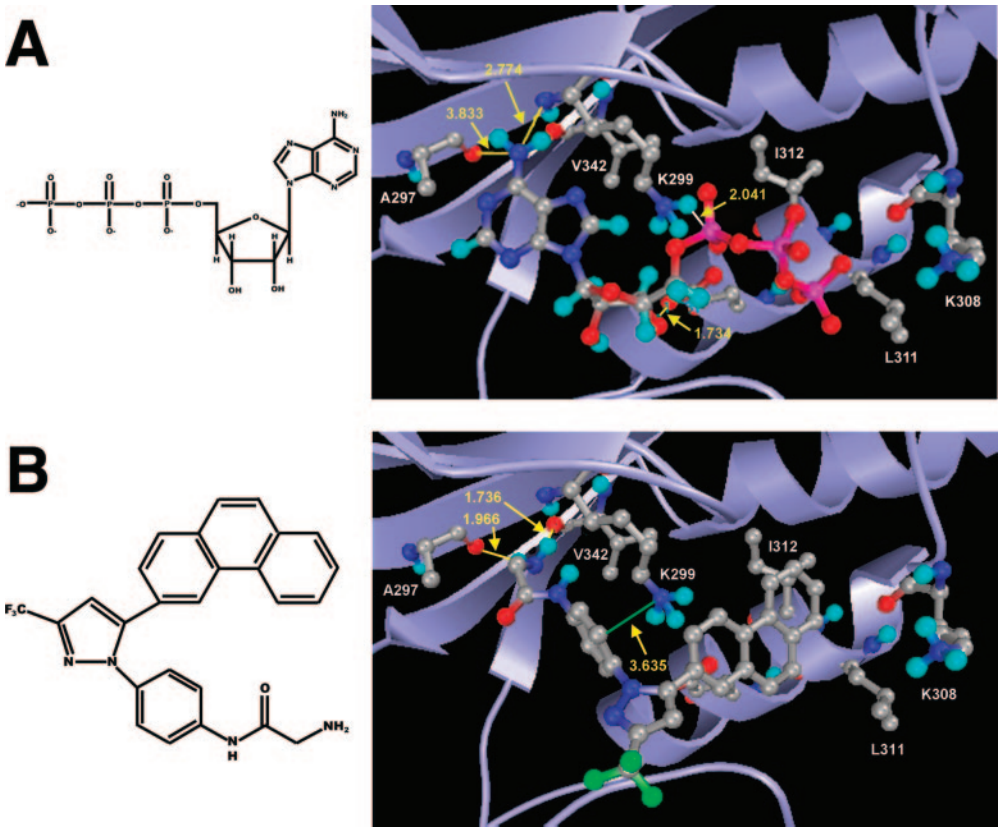

Fig. 4. Molecular modeling of potential OSU-03012 interactions with PAK 1. A, using the crystal structure of 1YHV (K229R, T432E) PAK1, the predicted structure of the wild-type PAK1 was obtained. The predicted docking of ATP into the binding pocket is demonstrated. B, the predicted docking of OSU-03012 into the PAK ATP binding domain is demonstrated. The PAK1 structure (modified 1YHV) is shown in ribbon form, and the ATP (A) and OSU-03012 (B) are presented as stick-and-ball structures, colored by atom types. The important amino acid residues are labeled with name and number. Hydrogen bonds are indicated in yellow. π-Cation interactions are depicted in green, and ionic interactions are in white. Distances for these interactions are labeled in yellow. In the structures of ATP and OSU-03012, gray is carbon; light blue/white is hydrogen; blue is nitrogen; red is oxygen; green is fluorine; and pink represents phosphorus. The chemical structures of ATP and OSU-03012 are shown on the left.

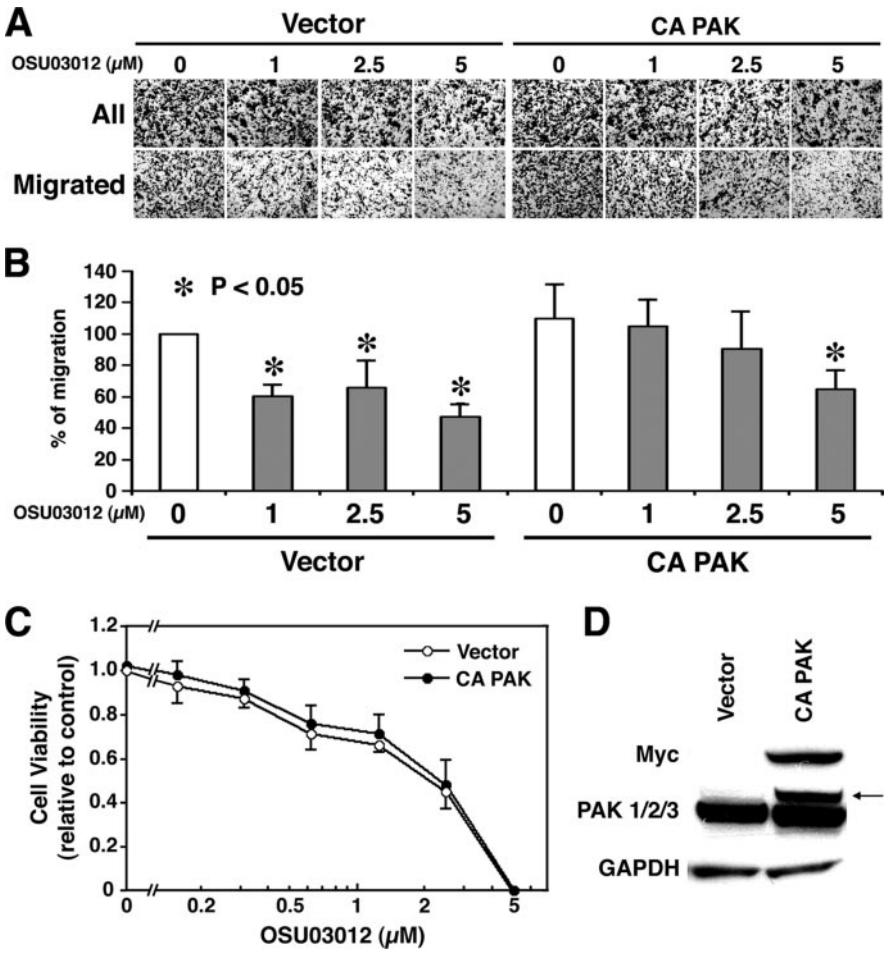

Fig. 5. OSU-03012 inhibition of NPA cell motility is partially PAK-dependent. NPA cells were transiently transfected with CA-PAK or vector and exposed to vehicle or OSU-03012. A and B, OSU-03012 inhibited migration of the vector-transfected cells at 1, 2.5, and 5 μM concentrations (*, $P < 0.05$ versus vehicle), whereas migration of the CA-PAK-transfected cells was blocked only by 5 μM OSU-03012 (*, $P < 0.05$ versus vehicle). The percentage of migration at the 1 and 2.5 μM doses was greater for the CA-PAK-transfectants than the control transfectants ($P < 0.01$). Mean values and S.D. are shown for quantitative results (B) from experiments performed in duplicate on three separate occasions. C, OSU-03012 effects on cell proliferation were not rescued by expression of CA-PAK. Results (mean and S.D.) are from experiments performed in triplicate on three separate occasions and were nonsignificant at all data points. D, expression of CA-PAK was confirmed by Western blot using anti-myc antibody and by the presence of a slower migrating band using anti-PAK1/2/3 (arrow).

findings in clinical samples. In breast cancer, increased expression and phosphorylation of PAK are associated with aggressive clinical behavior and the loss of response to antiestrogen therapies (Holm et al., 2006; Rayala et al., 2006). In addition, the ability of PAK1 to induce breast cancer in vivo was recently demonstrated (Wang et al., 2006). Moreover, PAK overexpression and activation has been implicated in the invasion and progression of a variety of others cancers (Kumar et al., 2006). Thus, PAKs seem to have a broad functional role in cancer; however, the role of PAK in thyroid cancer has not yet been defined.

In summary, we have established that OSU-03012, a derivative of celecoxib, inhibits PAK kinase. The effect of the compound on PAK activity occurs at similar or lower concentrations than PDK-1 based on in vitro kinase and cell-based assays, and both activities may be important in its biological effects. These data suggest that OSU-03012, or compounds with similar mechanisms of action, may represent new therapeutic tools to explore treatments for progressive malignancies associated with PAK overactivation.

Acknowledgments

We acknowledge Dr. Jonathan Chernoff for sharing constructs, providing scientific advice, and for critical review of the manuscript.

References

Alessi DR, Kozlowski MT, Weng QP, Morrice N, and Avruch J (1998) 3-Phosphoinositide-dependent protein kinase 1 (PDK1) phosphorylates and activates the p70 S6 kinase in vivo and in vitro. *Curr Biol* **8:**69–81.

Berman HM, Westbrook J, Feng Z, Gilliland G, Bhat TN, Weissig H, Shindyalov IN, and Bourne PE (2000) The Protein Data Bank. *Nucleic Acids Res* **28:**235–242.

Brader S and Eccles SA (2004) Phosphoinositide 3-kinase signalling pathways in tumor progression, invasion and angiogenesis. *Tumori* **90:**2–8.

Burridge K and Wennerberg K (2004) Rho and Rac take center stage. *Cell* **116:**167–179.

Chong C, Tan L, Lim L, and Manser E (2001) The mechanism of PAK activation. Autophosphorylation events in both regulatory and kinase domains control activity. *J Biol Chem* **276:**17347–17353.

Dong LQ, Zhang RB, Langlais P, He H, Clark M, Zhu L, and Liu F (1999) Primary structure, tissue distribution, and expression of mouse phosphoinositide-dependent protein kinase-1, a protein kinase that phosphorylates and activates protein kinase Cζ. *J Biol Chem* **274:**8117–8122.

Estour B, Van Herle AJ, Juillard GJ, Totanes TL, Sparkes RS, Giuliano AE, and Klandorf H (1989) Characterization of a human follicular thyroid carcinoma cell line (UCLA RO 82 W-1). *Virchows Arch B Cell Pathol Incl Mol Pathol* **57:**167–174.

Fagin JA, Matsuo K, Karmakar A, Chen DL, Tang SH, and Koeffler HP (1993) High prevalence of mutations of the p53 gene in poorly differentiated human thyroid carcinomas. *J Clin Invest* **91:**179–184.

Gatti A, Huang Z, Tuazon PT, and Traugh JA (1999) Multisite autophosphorylation of p21-activated protein kinase γ-PAK as a function of activation. *J Biol Chem* **274:**8022–8028.

Goodsell DS and Olson AJ (1990) Automated docking of substrates to proteins by simulated annealing. *Proteins* **8:**195–202.

Hofmann C, Shepelev M, and Chernoff J (2004) The genetics of Pak. *J Cell Sci* **117:**4343–4354.

Holm C, Rayala S, Jirstrom K, Stal O, Kumar R, and Landberg G (2006) Association between Pak1 expression and subcellular localization and tamoxifen resistance in breast cancer patients. *J Natl Cancer Inst* **98:**671–680.

Huber MA, Kraut N, and Beug H (2005) Molecular requirements for epithelial-mesenchymal transition during tumor progression. *Curr Opin Cell Biol* **17:**548–558.

King CC, Gardiner EM, Zenke FT, Bohl BP, Newton AC, Hemmings BA, and Bokoch GM (2000) p21-activated kinase (PAK1) is phosphorylated and activated by 3-phosphoinositide-dependent kinase-1 (PDK1). *J Biol Chem* **275:**41201–41209.

Kucab JE, Lee C, Chen CS, Zhu J, Gilks CB, Cheang M, Huntsman D, Yorida E, Emerman J, Pollak M, et al. (2005) Celecoxib analogues disrupt Akt signaling, which is commonly activated in primary breast tumours. *Breast Cancer Res* **7:**R796–R807.

Kulp SK, Yang YT, Hung CC, Chen KF, Lai JP, Tseng PH, Fowble JW, Ward PJ, and Chen CS (2004) 3-Phosphoinositide-dependent protein kinase-1/Akt signaling rep-

resents a major cyclooxygenase-2-independent target for celecoxib in prostate cancer cells. *Cancer Res* **64:**1444–1451.
Kumar R, Gururaj AE, and Barnes CJ (2006) p21-Activated kinases in cancer. *Nat Rev Cancer* **6:**459–471.
Lei M, Lu W, Meng W, Parrini MC, Eck MJ, Mayer BJ, and Harrison SC (2000) Structure of PAK1 in an autoinhibited conformation reveals a multistage activation switch. *Cell* **102:**387–397.
Lei M, Robinson MA, and Harrison SC (2005) The active conformation of the PAK1 kinase domain. *Structure* **13:**769–778.
Meier R and Hemmings BA (1999) Regulation of protein kinase B. *J Recept Signal Transduct Res* **19:**121–128.
Motti ML, Califano D, Troncone G, De Marco C, Migliaccio I, Palmieri E, Pezzullo L, Palombini L, Fusco A, and Viglietto G (2005) Complex regulation of the cyclin-dependent kinase inhibitor p27kip1 in thyroid cancer cells by the PI3K/AKT pathway: regulation of p27kip1 expression and localization. *Am J Pathol* **166:**737–749.
Rayala SK, Molli PR, and Kumar R (2006) Nuclear p21-activated kinase 1 in breast cancer packs off tamoxifen sensitivity. *Cancer Res* **66:**5985–5988.
Rosenfeld RJ, Goodsell DS, Musah RA, Morris GM, Goodin DB, and Olson AJ (2003) Automated docking of ligands to an artificial active site: augmenting crystallographic analysis with computer modeling. *J Comput Aided Mol Des* **17:**525–536.
Sahai E and Marshall CJ (2003) Differing modes of tumour cell invasion have distinct requirements for Rho/ROCK signalling and extracellular proteolysis. *Nat Cell Biol* **5:**711–719.
Saji M, Vasko V, Kada F, Allbritton EH, Burman KD, and Ringel MD (2005) Akt1 contains a functional leucine-rich nuclear export sequence. *Biochem Biophys Res Commun* **332:**167–173.
Scrutton NS and Raine AR (1996) Cation-pi bonding and amino-aromatic interactions in the biomolecular recognition of substituted ammonium ligands. *Biochem J* **319:**1–8.
Sells MA, Boyd JT, and Chernoff J (1999) p21-activated kinase 1 (Pak1) regulates cell motility in mammalian fibroblasts. *J Cell Biol* **145:**837–849.
Sells MA, Knaus UG, Bagrodia S, Ambrose DM, Bokoch GM, and Chernoff J (1997) Human p21-activated kinase (Pak1) regulates actin organization in mammalian cells. *Curr Biol* **7:**202–210.
Sells MA, Pfaff A, and Chernoff J (2000) Temporal and spatial distribution of activated Pak1 in fibroblasts. *J Cell Biol* **151:**1449–1458.
Storz P and Toker A (2002) 3′-Phosphoinositide-dependent kinase-1 (PDK-1) in PI 3-kinase signaling. *Front Biosci* **7:**d886–902.
Thiery JP (2002) Epithelial-mesenchymal transitions in tumour progression. *Nat Rev Cancer* **2:**442–454.
Vanhaesebroeck B and Alessi DR (2000) The PI3K-PDK1 connection: more than just a road to PKB. *Biochem J* **346:**561–576.
Vasko V, Espinosa AV, Scouten W, He H, Auer H, Liyanarachchi S, Larin A, Savchenko V, Francis GL, de la Chapelle A, et al. (2007) Gene expression and functional evidence of epithelial-to-mesenchymal transition in papillary thyroid carcinoma invasion. *Proc Natl Acad Sci U S A* **104:**2803–2808.
Vasko V, Saji M, Hardy E, Kruhlak M, Larin A, Savchenko V, Miyagawa M, Isozaki O, Murakami H, Tsushima T, et al. (2004) Akt activation and localization correlate with tumor invasion and oncogene expression in thyroid cancer. *J Med Genet* **41:**161–170.
Wang RA, Zhang H, Balasenthil S, Medina D, and Kumar R (2006) PAK1 hyperactivation is sufficient for mammary gland tumor formation. *Oncogene* **25:**2931–2936.
Yang Z, Rayala S, Nguyen D, Vadlamudi RK, Chen S, and Kumar R (2005) Pak1 phosphorylation of snail, a master regulator of epithelial-to-mesenchyme transition, modulates snail's subcellular localization and functions. *Cancer Res* **65:**3179–3184.
Zenke FT, King CC, Bohl BP, and Bokoch GM (1999) Identification of a central phosphorylation site in p21-activated kinase regulating autoinhibition and kinase activity. *J Biol Chem* **274:**32565–32573.
Zhao ZS and Manser E (2005) PAK and other Rho-associated kinases—effectors with surprisingly diverse mechanisms of regulation. *Biochem J* **386:**201–214.
Zhu J, Huang JW, Tseng PH, Yang YT, Fowble J, Shiau CW, Shaw YJ, Kulp SK, and Chen CS (2004) From the cyclooxygenase-2 inhibitor celecoxib to a novel class of 3-phosphoinositide-dependent protein kinase-1 inhibitors. *Cancer Res* **64:**4309–4318.

Address correspondence to: Dr. Matthew D. Ringel, 445 D McCampbell Hall, 1581 Dodd Drive, Columbus, OH 43210. E-mail: matthew.ringel@osumc.edu